HEFAT2007
5th International Conference on Heat Transfer, Fluid Mechanics and Thermodynamics
Sun City, South Africa
BM1

HYDROMAGNETIC SORET CONVECTION IN A SHALLOW POROUS ENCLOSURE WITH A SHEAR STRESS APPLIED ON THE FREE UPPER SURFACE

Bourich M.[(1)], Hasnaoui M.[(2)]*, Amahmid A.[(2)], Er-Raki M.[(2)] , Mamou. M.[(3)] and EL Ganaoui M.[(4)]
[(1)]Poly-disciplinary Faculty, Physics Department, Safi, Morocco
[(2)] Faculty of Sciences Semlalia, Physics Department, UFR TMF, Marrakesh, Morocco
[(3)] AL/IAR, National Research Council Canada, Ottawa, Ontario K1A 0R6, Canada
[(4)] University of Limoges, SPCTS UMR 66 38 CNRS, Faculty of Sciences and Techniques, Limoges, France
E-mail: hasnaoui@ucam.ac.ma

ABSTRACT

The fluid flow induced by combined effects of thermal gradient, thermal diffusion, magnetic field and an external shear stress in a horizontal porous layer, subject to uniform heat flux along its long horizontal walls is studied analytically and numerically. The shear stress is applied on the top horizontal free surface while the bottom one is assumed to be rigid. The problem formulation is based on the Brinkman model with the Boussinesq approximation. The governing parameters are the thermal Rayleigh number, R_T , the Lewis number, Le, the separation parameter, φ, the Darcy number, Da, the Hartmann number Ha, the dimensionless shear stress, τ and the aspect ratio of the enclosure, A_r. The analytical solution is derived on the basis of the parallel flow approximation and validated numerically using a finite difference method. The critical Rayleigh numbers for the onset of stationary, subcritical and oscillatory convection are determined explicitly as functions of the governing parameters for infinite layers in the absence of the external shear stress. The effect of the main governing parameters on the fluid flow and heat and mass transfer characteristics is discussed.

INTRODUCTION

Increasing attention is actually devoted by the researches to examine the effect of a magnetic field on natural convection induced in an electrically conducting fluid owing to its implication in many engineering applications. Metallurgical melting, solidification process, and the mechanism of crystals manufacturing are some examples concerned with convective flows under magnetic fields [1, 2]. The list of published papers on the subject, either in porous or fluid media, is very long. Therefore, the literature review is restricted here to some recent papers.

Paramagnetic fluid convection under a strong magnetic field in a cubical enclosure has been studied experimentally and numerically by Bednarz et al. [3]. The enclosure was heated from one vertical copper wall with electric wire and cooled from the opposite wall with water pumped from a thermo-stating bath. The working fluid is a glycerol aqueous solution containing a gadolinium nitrate hexahydrate to make it paramagnetic. It was observed that the increase of the magnetic induction leads to an intensification of the convection motion and to an improvement of heat transfer. Kaneda et al. [4] studied experimentally and numerically natural convection of liquid gallium under a uniform magnetic field with an external electric current. A cubic enclosure filled with the liquid metal was heated and cooled from the facing electro-conductive vertical sidewalls while other four walls were thermally and electrically insulated. The authors found that the magnetic field could lead to the suppression of the convection and the interaction between the magnetic field and the additional electric current induces the Lorenz force and affects the flow pattern and the heat transfer rate (depending on the combination of the external electric current and the direction of the magnetic field). Li and Stock [5] studied experimentally the natural convection of molten gallium in a cubic cell subject to a horizontal temperature gradient. They found that natural convection finished to be annihilated by increasing the applied field strength. The effect of the magnetic buoyancy forces on the convection in an inclined rectangular enclosure heated from one side and cooled from the opposite side has been examined by Ece et al. [6]. Their results show that the flow characteristics and the convective heat transfer depend strongly upon the strength and direction of the magnetic field, the aspect ratio and the inclination of the enclosure. In addition, the magnetic field significantly reduces the local Nusselt number by suppressing the convection currents.

The literature review shows that the existing works are mainly focused on the effect of magnetic field on pure thermal convection but the effect of a magnetic field on thermosolutal convection in the presence of Soret effect is much less

documented. Hence, the present paper is devoted to study analytically and numerically the combined effects of a magnetic field, the thermal diffusion, and an external shear stress on natural convection within an electrically conducting binary mixture confined in a horizontal porous enclosure heated from below.

NOMENCLATURE

A_r	(L′/H′)	Aspect ratio of the porous matrix
D	[m^2/s]	Mass diffusivity
D_T	[m^{2}K^{-1}/s]	Thermodiffusion coefficient
q'	[Wm^{-2}]	Constant heat flux density
D_a	[-]	Darcy number
R_T	[-]	Thermal Darcy-Rayleigh number
Le	[-]	Lewis number
Ha	[-]	Hartmann number
t	[-]	Dimensionless time

Special characters

α	[m^2/s]	Thermal diffusivity of the saturated porous medium
σ	[-]	Saturated porous medium to fluid heat capacity ratio
λ	[W/mK]	Thermal conductivity
φ	[-]	Separation parameter
ε	[-]	Normalized porosity of the porous medium

MATHEMATICAL MODEL

The configuration considered is a two-dimensional homogeneous horizontal porous layer of width L' and height H'. All boundaries of the porous matrix are assumed impermeable. The top and bottom horizontal walls are subjected to uniform fluxes of heat, q', while the vertical short walls of the porous layer are assumed adiabatic. A shear stress is applied on the top horizontal free surface while the bottom one is assumed to be rigid. A magnetic field of strength B is applied normal to the horizontal walls. The porous medium is considered isotropic, homogeneous and saturated with an electrically conducting binary fluid mixture obeying the Boussinesq approximation. Using the Brinkman model and the vorticity-stream function formulation, the dimensionless governing equations are stated as follows:

$$\nabla^2\Psi + Ha^2\frac{\partial^2\Psi}{\partial y^2} = Da\nabla^4\Psi - R_T\left(\frac{\partial T}{\partial x} + \varphi\frac{\partial S}{\partial x}\right) \quad (1)$$

$$\frac{\partial T}{\partial t} + u\frac{\partial T}{\partial x} + v\frac{\partial T}{\partial y} = \nabla^2 T \quad (2)$$

$$\varepsilon\frac{\partial S}{\partial t} + u\frac{\partial S}{\partial x} + v\frac{\partial S}{\partial y} = \frac{1}{Le}\left[\nabla^2 S - \nabla^2 T\right] \quad (3)$$

$$\nabla^2\Psi = -\zeta \quad (4)$$

$$u = \frac{\partial\Psi}{\partial y}, \qquad v = -\frac{\partial\Psi}{\partial x} \quad (5)$$

The dimensionless variables were obtained using the scales H', α/H', $\sigma H'^2/\alpha$ and α respectively for length, velocity, time and stream function. The remaining definitions are $T = (T' - T'_0)/\Delta T'$ and $S = S'/\Delta S'$ with $\Delta T' = q'H'/\lambda$ and $\Delta S' = -\Delta T' S'_0(1 - S'_0)D_T/D$; the prime denotes dimensional variables where the subscript 0 refers to the conditions at the origin of the coordinate system.

The hydrodynamic, thermal and concentration boundary conditions associated to the present problem are:

$$x = \pm\frac{A_r}{2},\ \Psi = 0,\quad \frac{\partial T}{\partial x} = \frac{\partial S}{\partial x} = 0 \quad (6a)$$

$$y = -\frac{1}{2},\quad \Psi = 0,\quad \frac{\partial T}{\partial y} = \frac{\partial S}{\partial y} = -1 \quad (6b)$$

$$y = \frac{1}{2},\quad \frac{\partial^2\Psi}{\partial y^2} = \tau,\quad \frac{\partial T}{\partial y} = \frac{\partial S}{\partial y} = -1 \quad (6c)$$

The heat and solute transfer across the layer are given in terms of the Nusselt and Sherwood numbers as:

$$Nu = \frac{1}{T(0,-1/2) - T(0,1/2)},\quad Sh = \frac{1}{S(0,-1/2) - S(0,1/2)}$$

Numerical Solution

The numerical solution of the full governing equations was obtained by using a central finite difference scheme, as described in Bourich et al. [7]. The vorticity, temperature and concentration equations, Eqs. (1)-(3), were solved iteratively in a time accurate mode using the alternate direction implicit method. At the boundaries, the values of the vorticity were calculated using Wood's relation (Roache [8]). Nodal values of the stream function were obtained, from equation (4), via a point successive-over-relaxation method. For large aspect ratio enclosures, a non-uniform grid was used in the horizontal direction in order to obtain a finer mesh in the end regions where strong gradient of temperature, concentration and velocity set in. A non-uniform grid was also used in the y-direction to solve the thin shear layers near the horizontal boundaries. The results reported in this paper were obtained with computations performed with a grid size of 121×61 for A_r=4 and 201×81 for $A_r \geq 8$.

Some typical numerical results, in terms of streamlines, isotherms and isosolutes contours, obtained within a shallow enclosure are illustrated in Fig. 1 for $R_T = 100$, Le=10, $Da = 0.1$, $\varphi = 0.5$, $\tau = 10$, Ha =1.5 and A_r = 8 . For large aspect ratio enclosures, the streamlines clearly shows that, the flow is parallel to the long active walls of the layer if we except the end regions. In addition, the isotherms and isosolutes show a horizontal linear stratification of both temperature and concentration. Based on these remarks, an analytical solution is developed in order to allow a parametric study which is very useful to understand the flow behavior.

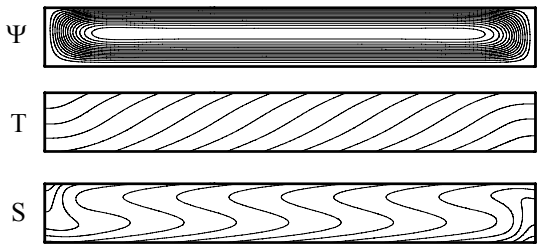

Figure1 Streamlines, isotherms and iso-concentration lines for R_T=100, Le=10, Da=0.1, Ha=1.5, φ=0.5, τ=10 and A_r=8

APPROXIMATE ANALYTICAL SOLUTION

The analytical solution was developed for steady-state flows in shallow enclosures using the parallel flow assumption [9], which led to the following approximations:

$\Psi(x,y) = \Psi(y)$, $T(x,y) = C_T x + \theta_T(y)$ and $S(x,y) = C_S x + \theta_S(y)$

where C_T and C_S are respectively unknown constant temperature and concentration gradients in the horizontal direction. Using the above approximations, together with the boundary conditions, equations (1)-(4) were reduced to a set of ordinary differential equations that can be solved to yield a closed form solution:

$$\Psi(y) = \frac{A}{\Omega^2}\cosh(\Omega y) + \frac{B}{\Omega^2}\sinh(\Omega y) + \frac{E_r}{2}y^2 + Cy + D$$

$$u(y) = \frac{A}{\Omega}\sinh(\Omega y) + \frac{B}{\Omega}\cosh(\Omega y) + E_r y + C$$

$$T(x,y) = C_T x - y + C_T f_\Omega(y)$$

$$S(x,y) = C_S x - y + (C_T + LeC_S) f_\Omega(y)$$

where

$$f_\Omega(y) = \left(\frac{A}{\Omega^3}\sinh(\Omega y) + \frac{B}{\Omega^3}\cosh(\Omega y) + \frac{E_r y^3}{6} + \frac{C}{2}y^2 + Dy \right)$$

$$E_r = -\frac{R_T(C_T + \varphi C_S)}{1 + Ha^2}\ ,\quad \Omega = \sqrt{\frac{1 + Ha^2}{Da}}$$

$$A = \frac{\tau(\Omega\cosh\frac{\Omega}{2} - 2\sinh\frac{\Omega}{2}) - \frac{E_r}{2}(\Omega^2\sinh\frac{\Omega}{2} + 2\Omega\cosh\frac{\Omega}{2} - 4\sinh\frac{\Omega}{2})}{\Omega\cosh\Omega - \sinh\Omega}$$

$$B = \frac{\tau\Omega\sinh\frac{\Omega}{2} - \frac{E_r}{2}(2\Omega\sinh\frac{\Omega}{2} - \Omega^2\cosh\frac{\Omega}{2})}{\Omega\cosh\Omega - \sinh\Omega}$$

$$C = \left(\frac{-2}{\Omega^2}\sinh(\frac{\Omega}{2})\right)B \text{ and } D = \left(\frac{-\cosh(\frac{\Omega}{2})}{\Omega^2}\right)A - \frac{E_r}{8}\ .$$

The expressions of C_T and C_S were determined by performing heat and solute balances across any transversal section of the porous layer [9]. This yields

$$C_T = \frac{-E_r G}{1 + E_r^2 H} \quad \text{and} \quad C_S = \frac{-E_r(1 + Le)G}{(1 + E_r^2 H)(1 + Le^2 E_r^2 H)}$$

where

$$G = C_1\left(\frac{\sinh(\Omega/2)}{\Omega^3} - \frac{\cosh(\Omega/2)}{2\Omega^2}\right) + \frac{1}{12}$$

$$H = \frac{1}{120} + C_1^2\left(\frac{-3\sinh(\Omega/2)\cosh(\Omega/2)}{4\Omega^5} + \frac{\cosh^2(\Omega/2)}{4\Omega^4} + \frac{1}{8\Omega^4}\right)$$

$$+ C_1\left(-\frac{2\sinh(\Omega/2)}{\Omega^5} + \frac{\cosh(\Omega/2)}{\Omega^4} - \frac{\cosh(\Omega/2)}{12\Omega^2}\right)$$

$$+ C_2^2\left(\frac{2\sinh^2(\Omega/2)}{\Omega^6} - \frac{3\sinh(\Omega/2)\cosh(\Omega/2)}{4\Omega^5} + \frac{\sinh^2(\Omega/2)}{12\Omega^4} - \frac{1}{8\Omega^4}\right)$$

with $C_1 = \frac{-2}{E_r}A$ and $C_2 = \frac{-2}{E_r}B$.

Then, Nu and Sh are given by:

$$Nu = \frac{1 + HE_r^2}{1 + (H - G^2)E_r^2}$$

$$Sh = \frac{1}{\frac{H - G^2}{H} + \frac{G^2(1 - HLeE_r^2)}{H(1 + HE_r^2)(1 + HLe^2E_r^2)}}$$

An equation for the constant E_r is established by substituting C_T and C_S in the expression of the latter (i.e. E_r) to obtain:

$$1 + H(1 + Le^2)E_r^2 + H^2Le^2E_r^4 - \frac{R_T G(HLe^2E_r^2 - (1 + \varphi(1 + Le))}{1 + Ha^2} = 0$$

The above equation can be solved numerically using the bisection method.

Case of $\tau = 0$

In the absence of the external shear stress ($\tau = 0$), the analytical resolution of the previous equation is possible and leads to:

$$E_r = \pm\left(\frac{-b \pm \sqrt{b^2 - 4Le^2c}}{2BLe^2}\right)^{\frac{1}{2}} \qquad (7)$$

with $b = \left(1 + Le^2\right) - \frac{GLe^2R_T}{1 + Ha^2}$ and $c = 1 - \frac{GR_T[1 + (1 + Le)\varphi]}{1 + Ha^2}$

In both situations where E_r is negative (clockwise flows) or positive (counter-clockwise flows), the Nusselt and Sherwood numbers remain the same. For convenience, only the solution corresponding to positive E_r will be considered. The solution with positive sign within the square root in equation. (7) will be denoted by E_{r+} and the solution with the negative sign by E_{r-}. These two solutions exist only when the following conditions are satisfied:

$$-b \pm \sqrt{b^2 - 4Le^2c} > 0 \quad \text{and} \quad b^2 - 4Le^2c > 0$$

Based on the above conditions it was demonstrated that the φ-Le plane can be divided into three regions exhibiting different behaviours. In the first region, stationary (i.e. supercritical convection) may exist. This region is defined by:

$$\varphi \geq \varphi_1(Le) = \frac{-1}{(1 + Le)(1 + Le^2)}$$

The critical Rayleigh number, R_{TC}^{sup}, above which the convective flow is possible is given by

$$R_{TC}^{sup} = \frac{1 + Ha^2}{G\,[\,1 + (1 + Le)\varphi\,]} \qquad (8)$$

In the second region both subcritical and stationary bifurcations are possible. This region is defined by

$$\frac{-1}{1 + Le} < \varphi < \frac{-1}{(1 + Le)(1 + Le^2)}$$

The expression of the critical Rayleigh number, R_{TC}^{sub}, for the onset of subcritical flows is given by:

$$R_{TC}^{sub} = \frac{(1 + Ha^2)(Le + 1)}{GLe^2}\left[Le - 1 - 2\varphi + 2\sqrt{-\varphi(Le - 1 - \varphi)}\,\right] \qquad (9)$$

In the third region, only the subcritical bifurcations are possible. This region is defined by

$$\varphi \le \varphi_2(Le) = \frac{-1}{1+Le}$$

The subcritical Rayleigh number for the third region is given by equation (9). However, for this region, both solutions E_{r^+} and E_{r^-} exist for any value of $R_T > R_{TC}^{sub}$.

For a shallow porous enclosure with an infinite aspect ratio, the onset of Hopf's bifurcation can be derived analytically as:

$$R_{TC}^{Hopf} = \frac{(\varepsilon Le+1)(1+Ha^2)}{GLe(\varepsilon+\varphi)} \qquad (10)$$

Equation (10) shows clearly that the occurrence of the oscillatory flow depends not only on Le ,φ, Da, and Ha (as it is the case for R_{TC}^{sub} and R_{TC}^{sup}) but also on ε.

RESULTS AND DISCUSSION

In the present study, the choice of the range of Darcy number was rather based on the literature review. Many authors have used values of Da as high as 0.1 (see for instance ref. [9]). In addition, the validity of the Brinkman model is largely discussed in the book by Nield and Bejan [10]; validity justified for porous media with large porosity (> 0.8).

Stability Diagram

Depending on the governing parameters of the problem, various regimes, with different flow behaviours, are found to exist. The stability diagram is used to analyze the flow behaviour and the nature of the existing bifurcations. Figure 2 shows a stability diagram obtained for $Le = 10$, $\varepsilon = 0.95$, $Da = 0.01$, $\tau = 0$ and $Ha = 1.5$. In this diagram, drawn in the $R_T - \varphi$ plane, four regions are delineated by the curves corresponding to R_{TC}^{sup}, R_{TC}^{sub} and R_{TC}^{Hopf} deduced from equations (8), (9) and (10), respectively. In region (I), below the subcritical Rayleigh number R_{TC}^{sub}, the fluid is expected to remain in an unconditionally stable motionless state in which any dynamic perturbation, regardless of its amplitude, decay with time. In region (II), between R_{TC}^{sub} and R_{TC}^{Hopf}, finite-amplitude convection exists and the rest state instability can be started only by large finite amplitude perturbations. The intersection between the thresholds of subcritical and stationary convection leads to a sub-codimension-2 point (represented in figure 2 by a triangle symbol). The sub-codimension-2 point results from the merging of subcritical and stationary bifurcations saddle-node points; it is localized by the following coordinates:

$$R_T^{sub-c2} = \frac{(1+Ha^2)(1+Le^2)}{GLe^2} \quad and \quad \varphi^{sub-c2} = \frac{-1}{(1+Le)(1+Le^2)}$$

In region (III), between R_{TC}^{Hopf} and R_{TC}^{sup}, persistent oscillatory or steady convection is possible depending essentially on the initial conditions used to start the numerical code. In the close vicinity of the Hopf's bifurcation threshold R_{TC}^{Hopf}, any small perturbation will grow in time in an oscillatory manner. The Hopf-codimension-2 point (intersection between the thresholds of Hopf and stationary convection) is indicated on the stability diagram (square symbol); its coordinates are given by:

$$R_T^{Hopf-c2} = \frac{(1+Ha^2)(\varepsilon Le(Le+1)+1)}{\varepsilon GLe(Le+1)-Le} \qquad (11)$$

$$and \quad \varphi^{Hopf-c2} = \frac{-1}{\varepsilon Le(Le+1)+1}$$

From equation (11), the onset of the overstability occurs for negative values of the separation coefficient ($-\varepsilon < \varphi < \varphi^{Hopf-c2}$). The oscillatory convection region extends to an upper limit where the oscillation frequency vanishes ($\omega = 0$). This line corresponds to the critical Rayleigh number $R_{TC}^{w=0}$, given by the following expression:

$$R_{TC}^{w=0} = \frac{(1+Ha^2)\left[\sqrt{-\varphi(\varepsilon(1+Le)-1)}+\sqrt{-\varepsilon(1-\varepsilon Le+\varphi)}\right]^2}{GLe(\varepsilon+\varphi)^2}$$

In region (IV), the fluid is unstable and any infinitesimal perturbation will initiate a convective flow.

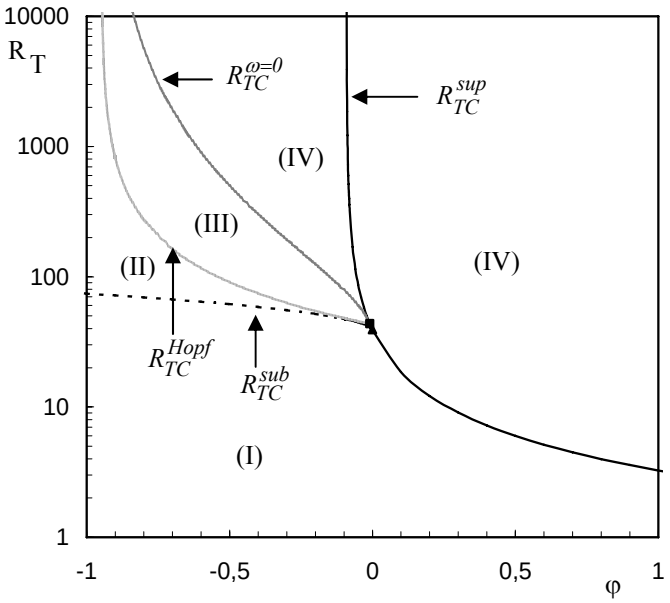

Figure2 Stability diagram for $Le = 10$, $\varepsilon = 0.95$, $Da = 0.01$, $\tau = 0$ and $Ha = 1.5$

Effect of Ha

The Hartmann number, Ha, is a measure of the magnetic buoyancy forces. It could be varied by changing the strength of the magnetic field or by considering various working electrically conducting fluids or different porous media with different permeabilities. Figure 3(a)-(c) shows the evolutions of the flow intensity, Ψ_0, the Nusselt number, Nu, and the Sherwood number, Sh, with Ha for $R_T = 200$, $Le = 10$, $Da = 0.01$, $\tau = 10$ and $\varphi = \pm 0.5$. The analytical solutions for Ψ_0, Nu and Sh, corresponding to the stable branches are seen to be in excellent agreement with the numerical ones obtained by solving the full governing equations. The results obtained

clearly show that the magnetic field has a strong effect on the fluid flow and heat and mass transfer characteristics. The value $\varphi = -0.5$ illustrates the case of subcritical convection for which both stable and unstable branches exist in the range $0 \le Ha \le Ha_{c1} = 2.932$. For $\varphi = 0.5$, which corresponds to supercritical convection, only the stable branch is existing and vanishes for $Ha > Ha_{c2} = 10.9$. For the stable branches, the increase of Ha induces a decrease of Ψ_0 and Nu (for both values of φ) indicating that the magnetic field reduces the flow intensity and the heat transfer. However, the evolution of Sh exhibits a different behaviour. For $\varphi = 0.5$, it goes through a maximum value $Sh_{max} \cong 6.92$ at $Ha_{max} \cong 3.4$, then decreases after that. For $\varphi = -0.5$, Sh increases globally with Ha for both stable and unstable solutions. It can be concluded from this section that the intensification of the magnetic field reduces considerably the heat transfer as it suppresses the motion and bring back the fluid to a purely diffusive regime.

Effect of τ

The variations of Ψ_0, Nu and Sh with the shear stress, τ, is illustrated in figure 4(a)-(c) for R_T =200, Le =10, Da = 0.1, $Ha = 2$ and $\varphi = \pm 0.5$. The results presented in this figure show the existence of two steady state solutions (characterized by one clockwise and one counter-clockwise circulations) in some range of τ which depends on φ. Theses solutions just exchange their roles when the sign of τ is changed. Therefore, the following discussion will be focused only on the range $\tau \ge 0$. In the absence of the shear stress applied on the top of the layer ($\tau = 0$), one of the two solutions is the mirror image of the other (across a vertical mirror), then they lead to the same values for $|\Psi_0|$, Nu and Sh. This feature is destroyed when the shear stress is not null and, consequently, one flow becomes more intense than the other depending on the sign of τ. Qualitatively, the curves of figure 4(a)-(c) present same trends for both values of φ. However, φ = 0.5 is more favourable to the persistence of the multiplicity of solutions when $|\tau|$ is increased. Also, the quantities Ψ_0 and Nu, corresponding to the counter-clockwise solution ($\Psi_0 > 0$), decrease with τ (the latter solution vanishes when τ exceeds the critical value $\tau_c = 17$ for φ = - 0.5 and $\tau_c = 61$ for φ = 0.5). However, these quantities increase with τ in the case of the clockwise solution. The curve of Sh exhibit complex behaviours; it undergoes a monotonic decrease or goes through a maximum then decreases after that when τ is increased above 0 and this, depending on the considered solution.

Conclusion

The effect of an applied magnetic field and an external shear stress on the Soret natural convection developed in a horizontal layer heated from below with a constant heat flux is conducted analytically and numerically. The shear stress is applied on the top horizontal free surface. The thresholds for subcritical, oscillatory and stationary convection are obtained explicitly as functions of the governing parameters for $\tau = 0$. The existence of a codimension-2 point is demonstrated and different flow regimes are delineated. The introduction of magnetic buoyancy forces, has a stabilizing effect on the system and reduces the flow intensity and heat transfer. However, it can engender an increase or a reduction of the mass transfer; depending on the values of Ha and the separation ratio. The application of a shear stress may suppress the multiplicity of solutions if τ is large enough. Furthermore, it enhances one flow and damps the other depending on the sign of τ.

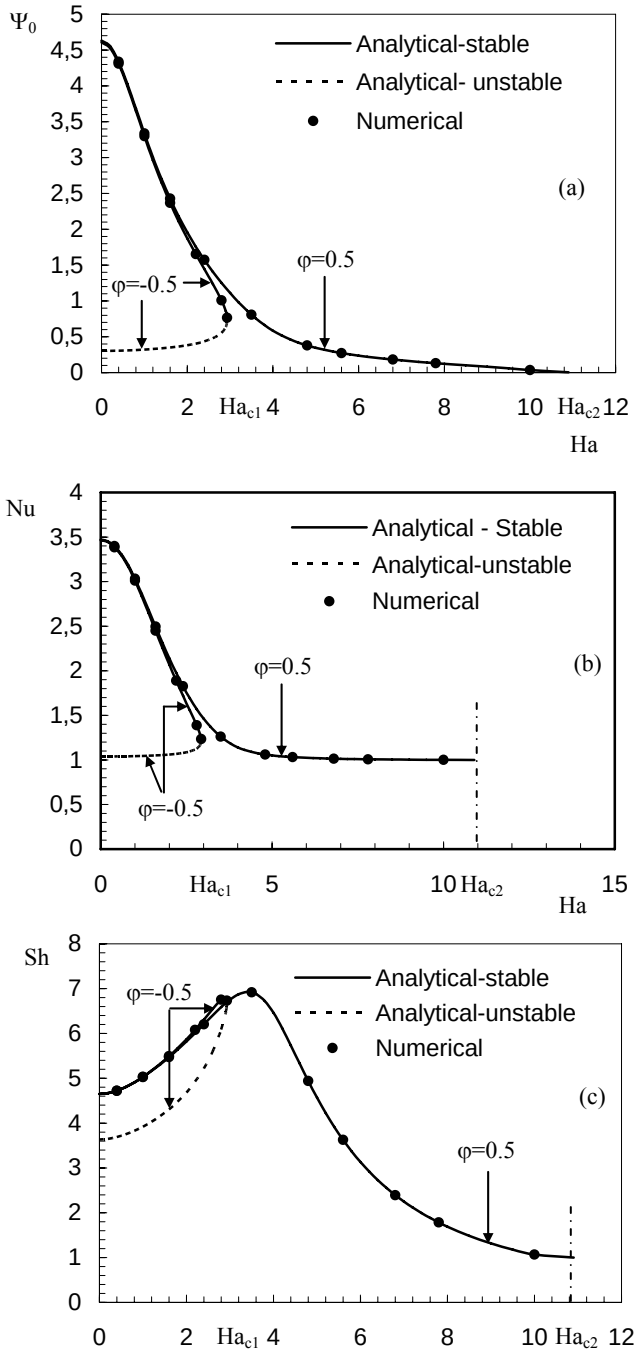

Figure3 Effect of Ha on (a)Ψ_0, (b) Nu and (c) Sh for R_T=200, Le=10, Da=0.01, τ =10 and $\varphi = \pm 0.5$.

REFERENCES

[1] Ezaki K., Kaneda M., Tagawa T. and Ozoe H., Numerical computation for the melt convection of the model system of continuous steel casting with various magnetic fields, *ISIJ Internat*, Vol. 43, 2003, pp. 907-914

[2] Sekar R., Vaidyanathan G., Hemalatha R. and Sendhilnathan S., Effect of spare distribution pores in a Soret-driven ferro thermohaline convection, *J. Magnetism and Magnetic Materiels*, Vol. 302, 2006, pp. 20-28

[3] Bednarz T., Fornalik E., Tagawa T., Ozoe H. and Szmyd J. S., Experimental and numerical analyses of magnetic convection of paramagnetic fluid in a cube heated and cooled from opposing verticals walls, *Int. J. Thermal Sciences*, Vol. 44, 2005, pp. 933-943

[4] Kaneda M., Tagawa T. and Ozoe H., Natural convection of liquid metal under a uniform magnetic field with an electric current supplied from outside, *Exp. Thermal Fluid Science*, Vol. 30, 2005, pp. 243-252

[5] Xu B., Li B. Q. and Stock D. E., An experimental study of thermally induced convection of molten gallium in magnetic fields, IJHMT, Vol. 49, 2006, pp. 2009-2019

[6] Ece M. C. and Büyük E., Natural-convection flow under a magnetic field in an inclined rectangular enclosure heated and cooled on adjacent walls, *Fluid Dynamics Research*, Vol. 44, 2005, pp. 933-943

[7] Bourich, M., Hasnaoui, M., Mamou, M. and Amahmid, A., Soret effect inducing Subcritical and Hopf bifurcations in a shallow enclosure filled with a clear binary fluid or a saturated porous medium: A comparative study, *Phys. Fluids*, Vol. 16, 2004, pp. 551-568

[8] Roache P.J., Computational fluid dynamics Hermosa, Albuquerque, NM, 1982

[9] Mamou M., Vasseur P. and Hasnaoui M., On Numerical Stability Analysis of Double-diffusive Convection in Confined Enclosures, *Journal of Fluid Mechanics*, Vol. 433, 2001, pp. 209-250

[9] Ettefagh J., Vafai K. and Kim S.J., Non-Darcian effects in open-ended cavities filled with a porous medium, Transactions of the ASME, *Journal of Heat Transfer*, vol. 113, 1991, pp. 747-756.

[10] Nield D.A. and Bejan A., Convection in porous media, 1992, *Springer-Verlag*.

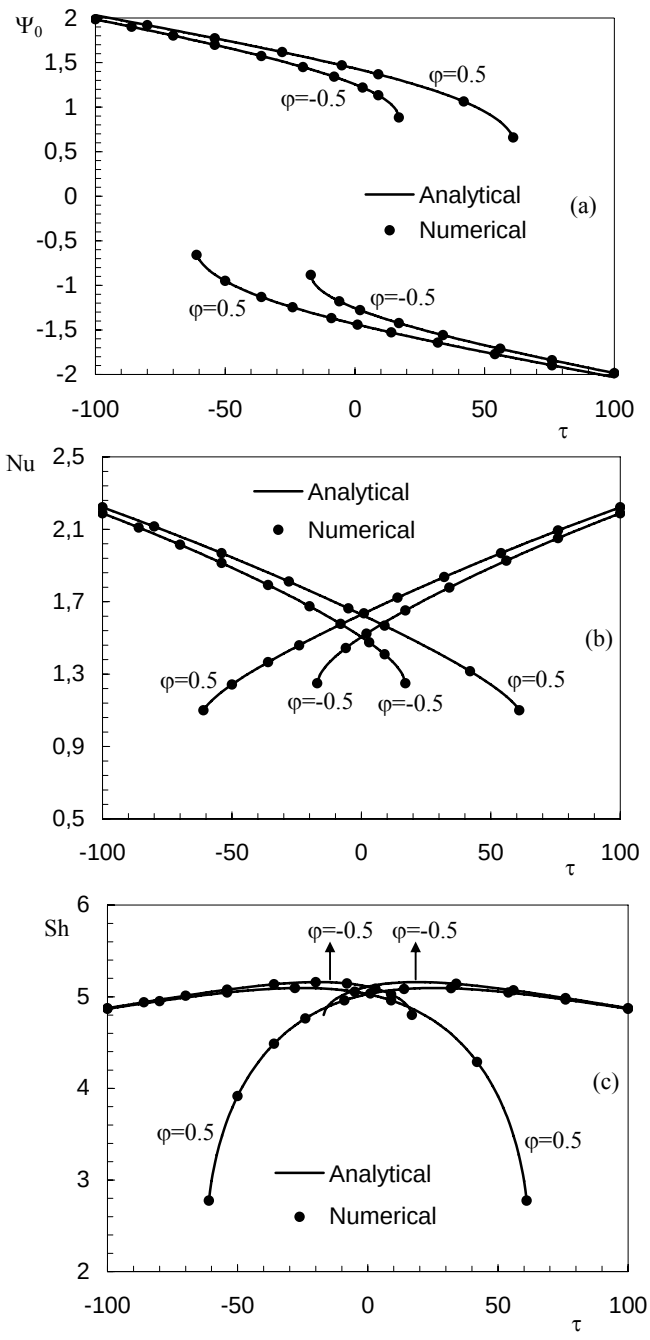

Figure4 Effect of τ on (a) Ψ_0, (b) Nu and (c) Sh for R_T=200, Le=10, Da=0.1, Ha=2 and φ = ± 0.5.